

AD610954

MEMORANDUM

ARM-4388

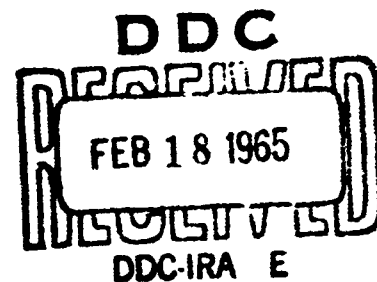
FEBRUARY 1965

TRANSMISSION OF MICROPULSATIONS THROUGH THE LOWER IONOSPHERE

Carl Greifinger and Phyllis Greifinger

COPY <u>2</u> OF <u>3</u> <u>R</u>	
HARD COPY	\$. 2.00
MICROFICHE	\$. 0.50

47P



The RAND Corporation
SANTA MONICA • CALIFORNIA

ARCHIVE COPY

AD610954

MEMORANDUM

RM-4388

FEBRUARY 1965

**TRANSMISSION OF MICROPULSATIONS
THROUGH THE LOWER IONOSPHERE**

Carl Greifinger and Phyllis Greifinger

DDC AVAILABILITY NOTICE

Qualified requesters may obtain copies of this report from the Defense Documentation Center (DDC).

Approved for ODS release

The **RAND** *Corporation*

1700 MAIN ST. • SANTA MONICA • CALIFORNIA • 90406

PREFACE

This report is part of RAND's continuing interest in the detection of high-altitude nuclear explosions. In particular, it is concerned with the low-frequency hydromagnetic waves which are generated by such explosions, and which are detected by ground-current measurements at world-wide locations. In this report, we direct our attention to the response of the ionosphere to such low-frequency hydromagnetic disturbances. The purpose is to separate the effects of the medium from those of the source on the transmitted disturbance.

SUMMARY

In this report, we study the propagation through the ionosphere of sub-extremely-low frequency (< 0.1 cps) hydromagnetic waves. We consider the case of plane wave propagation in the vertical direction in the presence of a uniform magnetic field which is also in the vertical direction (so-called polar propagation). The purpose is to separate out the effects of the ionosphere on hydromagnetic disturbances propagating through it. The ionosphere is assumed to extend infinitely far in the upward direction and to terminate abruptly 80 km above a perfectly conducting flat earth. The charged particle density is assumed to be constant throughout the ionosphere, and the neutral particle density to vary exponentially with altitude. The coupled hydrodynamic and electromagnetic equations for the medium are linearized, and, with the approximations valid for low-frequency waves, the resulting system is shown to reduce to a second-order wave equation. A steady-state solution of this equation is obtained, from which transmission and reflection coefficients are calculated. It is found that, for ionospheric conditions corresponding to daytime at sunspot maximum, the transmission coefficient exhibits a pronounced resonance at a frequency of about 0.015 cps. Since this is approximately the frequency of so-called Pc oscillations, it is suggested that the resonance just described accounts for these natural micropulsations in the geomagnetic field. It is found that the resonance shifts to higher frequencies at night, also in agreement with the data on natural Pc oscillations. It is shown that the presence of an almost perfectly conducting ground (at these frequencies) is important in determining the location of the resonance. Finally, it is shown that disturbances reaching the ground, in the polar regions, should be very nearly left-circularly polarized.

ACKNOWLEDGMENTS.

The authors are very much indebted to Dr. E. C. Field of The RAND Corporation for many helpful discussions. We are also grateful to Prof. H. Booker of Cornell University for pointing out the quarter-wave plate analogy in the case of the grounded ionosphere.

CONTENTS

PREFACE	iii
SUMMARY	v
ACKNOWLEDGMENTS	vii
Section	
I. INTRODUCTION	1
II. WAVE EQUATION IN THE IONOSPHERE	6
III. IONOSPHERIC "REGIONS"	11
IV. SOLUTION OF THE WAVE EQUATION FOR A MODEL IONOSPHERE	13
V. TRANSMISSION AND REFLECTION COEFFICIENTS	20
APPENDIX	39
REFERENCES	42

I. INTRODUCTION

A subject which has been receiving considerable attention for a long time is the existence of sub-extremely-low frequency fluctuations in the geomagnetic field. These fluctuations, which have periods of the order of seconds to tens of seconds, are associated with many naturally occurring geomagnetic phenomena, and have also been generated by nuclear explosions at high altitude.

The experimental data on natural field fluctuations have been summarized by Campbell (1963). Briefly, the data show regular oscillations in the frequency range below about 0.2 cps appearing over broad sections of the earth with related phase on days of high solar-terrestrial activity. The oscillations appear quite sinusoidal, with a period which varies slightly with season and considerably with the time of day; longer period oscillations are observed near noon whereas shorter periods are noted at night. Maple (1959), for example, found two daytime bands of oscillations centered at 70 seconds and 20 seconds, respectively, and a nighttime band with an average period of 8 seconds. The polarization of the magnetic field is elliptical in the horizontal plane. The signal amplitude shows a latitude dependence, dropping off toward lower latitude by a factor of about $\frac{1}{2}$ per 20° to 30° lower latitude.

In addition to the data on natural fluctuations, much data exists on the fluctuations generated by various high-altitude nuclear explosions. This data shows a striking similarity between bomb-generated and natural fluctuations in two important respects. In the first place, the initial phase of signals generated by such explosions arrives essentially simultaneously at stations all over the world (with time delays after detonation which depend on the altitude of the explosion). Secondly, the signals generated by a given explosion are essentially the same in shape and duration at stations all over the world. In general, one may say that the signals resulting from low-yield detonations, such as the Argus series, are quite similar in most respects to naturally occurring signals.

One further point of interest is the power spectra associated with oscillations in this frequency range. Several authors (Santirrocco and Parker, 1963; Smith, Provazek and Bostick, 1961; Campbell, 1959; and Horton and Hoffmann, 1962) have analyzed the spectra associated with natural fluctuations, while Hodder (1963) has presented a spectral analysis of signals resulting from nuclear explosions as well as of the natural background. These analyses show one or more large peaks in the frequency range of interest. In particular, a large fraction of Hodder's spectra, both bomb-induced and naturally occurring, show a very prominent peak at about .02 cps.

The simultaneity of arrival of these fluctuations over broad sections of the earth has led many authors to conclude that the signals received at various stations arise from a common ionospheric disturbance. The disturbance is generally believed to propagate through the ionosphere as a hydromagnetic wave which, upon emergence from the ionosphere, propagates as an electromagnetic signal to the various points of detection. The time delay between detonation and receipt of explosion-generated signals would then represent the transit time of the hydromagnetic disturbance through the ionosphere. Estimates of these transit times are in reasonable agreement with the observed delays.

The point which concerns us in this paper is the striking similarity among signals in this frequency range resulting from a variety of natural causes, and the similarity between these natural signals and those which are produced by explosions. These similarities have suggested to many authors the importance of the ionosphere in the transmission of such disturbances. We would point out here that the similarity between natural fluctuations, which are generated, for the most part, outside the ionosphere, and explosion-produced fluctuations, which are generated in the ionosphere itself, emphasizes the particular importance of the lower ionosphere (below about 400 or 500 km) in determining the characteristics of the observed signals. It is this region of the ionosphere to which we turn our attention.

The low-frequency transmission characteristics of the lower ionosphere have been investigated by Francis and Karplus (1960) and by Field (1963). The former, making certain simplifying assumptions, numerically integrated the differential equations for the propagation of hydromagnetic disturbances in the ionosphere, using empirical ionospheric properties, chosen to correspond to the daytime at sunspot maximum. Their numerical results show that the ionosphere is essentially transparent for angular frequencies somewhat less than 1 radian/sec. Field (1963) used empirical ionospheric properties to calculate an altitude-dependent complex index of refraction for the ionosphere. He then approximated the ionosphere by two layers, the upper of which has a real index of refraction and the lower of which has a complex index of refraction, and calculated the resulting transmission coefficient. Field's results are substantially in agreement with those of Francis and Karplus (1960). Neither investigation, however, revealed any prominent resonances in the transmission coefficient.

In this paper, we also calculate the transmission and reflection coefficients for the lower ionosphere. We use essentially the same model as Francis and Karplus (1960), but with some additional simplifications which make possible an analytic, rather than a numerical, solution. The advantages of an analytic solution lie, of course, in the physical insight it provides and in the ease with which the effects of a variation in ionospheric parameters can be determined. Even with the necessary simplifications, the important features of the phenomenon appear in such a model.

We start by incorporating our simplifying assumptions into the basic equations of motion for the ionospheric constituents. From these basic equations we derive a wave equation, which we then examine in the frequency region below about 1 cps for the case of polar propagation. We show that, for the polar propagation of hydromagnetic waves in this frequency range, the ionosphere consists essentially of three "regions": a lossless "Alfvén region," above about 350 km, in which the disturbance propagates as a pure Alfvén wave, a "Hall region," below about 130 km, which is dominated by

ion-neutral particle collisions and in which the propagation characteristics are quite different from the Alfvén region, and an intervening "transition region" which smoothly connects the Alfvén and Hall regions. (We shall sometimes refer to the Alfvén region as the "upper ionosphere," and to the transition and Hall regions as the "lower ionosphere.") We then assume that the Alfvén speed is uniform throughout the entire (semi-infinite) ionosphere and that the ion-neutral particle collision frequency (which enters only in the transition region) varies exponentially with altitude. With these assumptions, we are able, without the further introduction of any artificial boundaries, to obtain an analytic solution of the wave equation. The solution immediately yields the desired transmission and reflection coefficients. The transmission coefficient is found to exhibit a pronounced resonance at a frequency of .015 cps for daytime conditions, with an upward shift in frequency for nighttime conditions. This resonance is in the frequency range of so-called Pc oscillations, which are therefore apparently accounted for by the filtering action of the lower ionosphere. (This resonance does not appear in the work of Francis and Karplus (1960), whose calculations extend only to a frequency of 1 rad/sec at the low end, nor in the work of Field (1963) who was concerned only with an average transmission coefficient rather than in its detailed dependence on frequency.)

It should be mentioned that our assumption of a constant Alfvén speed throughout a semi-infinite ionosphere treats the upper ionosphere as a lossless, non-dispersive medium (or transmission line). It is known, however, that the Alfvén speed actually increases with altitude in the region between about 200 km and 2000 km. This should be of little consequence for the initial phase of bomb-induced signals which are generated at altitudes of a few hundred kilometers, but may be expected to modify signals which are generated at altitudes of 2000 km or more. The transmission properties of a medium with varying Alfvén speed have been investigated by several authors. Jacobs and Watanabe (1962) have considered the case of a collisionless upper ionosphere in which the Alfvén speed increases

exponentially with altitude to a maximum at 2000 km. They approximated the medium by six uniform Alfvén layers of equal thickness, the lowest of which is grounded, and numerically calculated a transmission coefficient. Field (1964) has obtained an analytic solution to the same problem. These authors find that a filtering action takes place between the region of maximum velocity at around 2000 km and the bottom of the upper ionosphere. Various resonances appear, the lowest of which occurs at a frequency of about .1 cps, or about an order of magnitude higher than the frequency of the resonance associated with the lower ionosphere. Prince and Bostick (1964) have carried out numerical calculations using a more realistic ionosphere, with various collisional effects taken into account. They find similar resonances in the transmission coefficient. These resonances in the transmission coefficient of the upper ionosphere are thought to be responsible for "pearl" type oscillations.

For disturbances originating at heights of 2000 km or more (and in the frequency range below about 1 cps), the ionosphere below 2000 km therefore appears very much like two successive filters. The upper filter has a transmission resonance at about .1 cps, and the lower filter a transmission resonance at about .015 cps. The combined transmission coefficient is essentially the product of the separate transmission coefficients.

II. WAVE EQUATION IN THE IONOSPHERE

We start by making the same simplifying assumptions as Francis and Karplus (1960), viz.,

- (1) the static magnetic field is uniform,
- (2) the pressure is so low that hydrostatic restoring forces and gravitational forces are small compared to electrostatic restoring forces,
- (3) the fractional ionization is so small that collisions between electrons and ions may be neglected,
- (4) the fractional ionization is so small that collisions of neutrals with charged particles may be neglected (i.e., the neutrals do not participate in the mass motion), and
- (5) the ionosphere is still and flat, and the wave normal is along the ionospheric density gradient.

In addition to these assumptions, we further assume that

(6) the static field is uniform and in the vertical direction, which restricts the applicability of our model, in detail at least, to the polar and auroral regions. These basic assumptions will now be incorporated into the equations of motion for the ionospheric constituents.

We start with the following transport equations for the electrons and (singly-charged) ions:

$$\frac{\partial \vec{v}_e}{\partial t} + \vec{v}_e \cdot \nabla \vec{v}_e + \frac{e}{m_e} (\vec{E} + \frac{\vec{v}_e \times \vec{B}}{c}) = -\nu_e \vec{v}_e \quad (1a)$$

$$\frac{\partial \vec{v}_i}{\partial t} + \vec{v}_i \cdot \nabla \vec{v}_i - \frac{e}{m_i} (\vec{E} + \frac{\vec{v}_i \times \vec{B}}{c}) = -\nu_i \vec{v}_i, \quad (1b)$$

where ν_e and ν_i are the collision frequencies of electrons with neutrals and ions with neutrals, respectively, and the other symbols have their usual meanings. (We shall use cgs units throughout.) If we take the positive z-direction to be vertically downward and

restrict our attention to plane transverse waves of small amplitude, we may write

$$\vec{v} = (v_1, v_2, 0) \quad (2a)$$

$$\vec{B} = (b_1, b_2, B_0) \quad (2b)$$

$$\vec{E} = (E_1, E_2, 0) \quad (2c)$$

where the v , b , and E are assumed to be small quantities. Linearizing the transfer equations, we obtain

$$\frac{\partial \vec{v}_e}{\partial t} + \omega_e \vec{v}_e \times \vec{e}_3 + v_e \vec{v}_e = - \frac{e}{m_e} \vec{E} \quad (3a)$$

$$\frac{\partial \vec{v}_i}{\partial t} - \omega_i \vec{v}_i \times \vec{e}_3 + v_i \vec{v}_i = \frac{e}{m_i} \vec{E} \quad (3b)$$

where \vec{e}_3 is a unit vector in the positive z -direction, and $\omega_{e,i} = \frac{e B_0}{m_{e,i} c}$ is the cyclotron frequency of the particular ionospheric component. With the assumption of a static field in the vertical direction, an essential simplification of the equations results if we introduce the complex variables

$$v = v_1 - i v_2 \quad (4a)$$

$$E = E_1 - i E_2 \quad (4b)$$

In terms of these variables, Eqs. (3a) and (3b) take the form

$$(\Omega_e + i \omega_e) v_e = - \frac{e}{m_e} E \quad (5a)$$

$$(\Omega_i - i \omega_i) v_i = \frac{e}{m_i} E \quad (5b)$$

where Ω is the operator

$$\Omega \equiv \frac{\partial}{\partial t} + v \quad (6)$$

for the component in question.

Remembering that the current density is defined as

$$\vec{j} = n e (\vec{v}_i - \vec{v}_e) \quad (7)$$

where n is the number density of electrons and ions (assumed equal), we may combine Eqs. (5a) and (5b) to obtain

$$(\Omega_e + i\omega_e)(\Omega_i - i\omega_i) \vec{j} = e \left[\frac{1}{m_i} (\Omega_e + i\omega_e) + \frac{1}{m_e} (\Omega_i - i\omega_i) \right] \vec{E} \quad (8)$$

where

$$\vec{j} = j_1 - i j_2. \quad (9)$$

We note, in passing, that Eq. (8) provides a very simple derivation of two of the diagonal components, σ_1 and σ_2 , of the conductivity tensor. The equation defining the conductivity tensor reduces, in the present case, to

$$\vec{j} = \sigma_1 \vec{E} + \sigma_2 \vec{E} \times \vec{e}_3 \quad (10)$$

which may also be written

$$\vec{j} = (\sigma_1 + i \sigma_2) \vec{E}. \quad (11)$$

Assuming a time dependence of the form $e^{-i\omega t}$ in Eq. (8), and comparing Eqs. (8) and (11), we obtain

$$\sigma_1 = n e^2 \left\{ \frac{v_e - i\omega}{m_e [(v_i - i\omega)^2 + \omega_e^2]} + \frac{v_i - i\omega}{m_i [(v_i - i\omega)^2 + \omega_i^2]} \right\} \quad (12a)$$

$$\epsilon_2 = n e^2 \left\{ - \frac{\omega_e}{m_e [(v_e - i\nu)^2 + \omega_e^2]} + \frac{\omega_i}{m_i [(v_i - i\nu)^2 + \omega_i^2]} \right\}, \quad (12b)$$

in agreement with the usual formulas for these conductivities.

Finally, to derive a wave equation for E , we combine Eq. (8) with Eq. (7) and

$$\nabla^2 E = \frac{4\pi}{c^2} \frac{\partial j}{\partial t} \quad (13)$$

to obtain

$$(\Omega_e + i\omega_e)(\Omega_i - i\omega_i) \nabla^2 E = \frac{4\pi n e^2}{m_e m_i c^2} (m_e \Omega_e + m_i \Omega_i) \frac{\partial E}{\partial t} \quad (14)$$

where we have used $m_e \omega_e = m_i \omega_i$. The general wave equation is evidently a complicated fourth-order equation and we shall not attempt to discuss its general properties at this time. We do note, however, that in the limit of very strong magnetic field and no collisions, i.e., $\omega_e, \omega_i \rightarrow \infty$ and $\nu_e, \nu_i \rightarrow 0$, Eq. (14) reduces to the usual equation for Alfvén waves

$$\nabla^2 E = \frac{1}{v_a^2} \frac{\partial^2 E}{\partial t^2}, \quad (15)$$

where $v_a^2 = \frac{B_0^2}{4\pi n(m_i + m_e)}$ is the square of the Alfvén speed.

Fortunately, for the frequency regime under consideration, Eq. (14) simplifies considerably. Much of the simplification results from the properties of the ionosphere in the region of interest (80 km - 500 km), viz.,

$$(a) \quad \omega_e \sim 10^6 \text{ rad/sec},$$

$$(b) \quad 10^2 < \nu_e < 10^5 \text{ rad/sec},$$

$$(c) \quad \omega_i \sim 10^2 \text{ rad/sec},$$

$$(d) \quad 10^{-2} < \nu_i < 10^4 \text{ rad/sec}.$$

(See Francis and Karplus (1960) for a tabulation of ionospheric properties). In view of these relationships, and the fact that we are interested in frequencies $\omega \ll \omega_i$ (i.e., $\frac{\partial}{\partial t} \ll \omega_i$), the following approximations become valid:

$$\Omega_e + i\omega_e \approx i\omega_e \quad (16a)$$

$$\Omega_i - i\omega_i \approx \nu_i - i\omega_i. \quad (16b)$$

Furthermore, since $\nu_i \gtrsim \left(\frac{m_e}{m_i}\right)^{\frac{1}{2}} \nu_e$,

$$m_e \Omega_e + m_i \Omega_i \approx m_i \Omega_i \quad (16c)$$

to terms of relative order $(m_e/m_i)^{\frac{1}{2}}$. With these approximations, Eq. (14) becomes

$$(\nu_i - i\omega_i) \nabla^2 E = -i\omega_i \frac{1}{v_a} \Omega_i \frac{\partial E}{\partial t}, \quad (17)$$

a somewhat more tractable second-order equation.

III. IONOSPHERIC "REGIONS"

Before attempting a solution of Eq. (17), it is worth noting that for hydromagnetic waves in the frequency regime below about 1 cps, the ionosphere consists of three essentially distinct regions, which are characterized by the relative magnitudes of the three frequencies ν_i , ω_i , and ω (the angular frequency of the disturbance). In order of increasing altitude, these regions are:

(a) Hall Region - This is defined to be the region in which the inequality $\omega \ll \omega_i < \nu_i$ is satisfied, i.e., where the collision frequency is the dominant frequency. It lies, therefore, between about 80 km and 130 km. The boundaries of this region are independent of ω , provided that $\omega \ll \omega_i$. Here, the Hall effect predominates; in terms of the conductivities defined by Eqs. (11a) and (11b), $\sigma_2 \gg \sigma_1$. In this region, Eq. (17) reduces to

$$\nabla^2 E = -i \frac{\omega_i}{\nu_a} \frac{\partial E}{\partial t}, \quad (18)$$

i.e., to a Schrödinger-like equation. It is important to note that, though this region is collision-dominated, the wave equation nevertheless does not contain the collision frequency explicitly. The implicit importance of collisions is, however, reflected in the form of the equation.

(b) Transition Region - This region is defined by the inequality $\omega < \nu_i < \omega_i$. It lies between about 130 km and 350 km. The location of the upper boundary of this region depends on the frequency ω ; the value given is appropriate to a frequency $\omega \approx .3$ rad/sec. Here no further simplification of the wave equation is possible; collisions thus play an explicit role in this region.

(c) Alfvén Region - This is the region in which the inequality $\nu_i < \omega \ll \omega_i$ is satisfied. It is therefore the region above about 350 km, and in our model is assumed to be semi-infinite in extent. In this region, Eq. (17) reduces to Eq. (14), the usual equation for Alfvén waves. The wave equation, in this region, is independent of the collision frequency.

The essential point of the preceding discussion is that the actual functional form of the collision frequency enters only in the transition region. To obtain an analytic solution to the wave equation, we must, of course, approximate the ionospheric collision frequency by an analytic function. To obtain an analytic approximation which is valid over a large region of the ionosphere, and which at the same time permits an analytic solution of the wave equation, does not seem possible. We see, however, that this is fortunately not necessary; we are presented with the far simpler task of constructing an expression which is a good approximation only over a relatively limited portion of the ionosphere.

Finally, let us emphasize that we have been speaking of "regions" in a qualitative rather than in a mathematical sense. In the model which we employ below, it will not be assumed that these regions are separated by artificial sharp boundaries, with a separate wave equation appropriate to each. The single wave equation, E_1 (17), will govern the propagation of the disturbance throughout the entire ionosphere. The essence of the above discussion is that the character of the wave equation changes (continuously, of course) from one region to the next, and this property will obviously be reflected in the solution to that equation.

IV. SOLUTION OF THE WAVE EQUATION FOR A MODEL IONOSPHERE

In this section we shall construct the steady-state solution to Eq. (17) for a model ionosphere which will be described below. If we introduce a time dependence of the form $e^{-i\omega t}$, Eq. (17) becomes

$$\frac{d^2 E}{dz^2} + \frac{\omega^2}{c^2} n^2(\omega; z) E = 0 \quad (19)$$

where

$$n^2(\omega; z) = \frac{c^2}{v_a^2} \frac{\omega_i}{\omega} \frac{(1 - i\omega/v_i)}{(1 - i\omega_i/v_i)} \quad (20)$$

In Eq. (19), E now denotes $E(z, \omega)$, the Fourier transform of $E(z, t)$. With a time dependence of the form $e^{-i\omega t}$ and the definition of $E(z, t)$ by Eq. (4b), positive values of ω correspond to left-circularly polarized waves, which we shall call the L-mode, and negative values of ω correspond to right-circularly polarized waves, which we shall call the R-mode. (In the case of polar propagation which we are considering, these two modes are decoupled from each other.)

The more important properties of our three regions can already be deduced from Eqs. (19) and (20). In the Alfvén region, $\omega/v_i \gg 1$ and $\omega_i/v_i \gg 1$, so that the index of refraction $n(\omega; z)$ becomes

$$n(\omega; z) \rightarrow n_a = \frac{c}{v_a} \quad (21)$$

This is the well-known result that, for both modes of propagation, the Alfvén region is a lossless and non-dispersive medium.

In the Hall region, $\omega/v_i \ll 1$ and $\omega_i/v_i \ll 1$, and the index of refraction becomes

$$n(\omega; z) \rightarrow n_H(\omega) = \left(\frac{\omega_i}{\omega}\right)^{\frac{1}{2}} \quad (22)$$

This medium therefore appears quite different to the two modes of propagation. For the L-mode ($\omega > 0$), the index of refraction is real, and this mode therefore propagates through the Hall region without attenuation, but obviously with dispersion. For the R-mode ($\omega < 0$), the situation is quite different; the index is pure imaginary, and this mode is consequently evanescent. Because of this, the transmission coefficient for the R-mode drops off very rapidly with frequency, and it is mainly the L-mode which gets through the ionosphere. The disturbances reaching the ground should thus be circularly polarized. (We must remember, of course, that we are treating the case of polar propagation; in the higher latitude, but non-polar, regions, we would expect the same mechanism to produce elliptical polarization, in agreement with observation.)

In the transition region, no similar simplification of the index of refraction takes place. The index for both modes is complex, so that in this region each mode undergoes both attenuation and dispersion.

The quantities ν_i , ω_i , and ν_a^2 in Eq. (19) are, of course, all functions of the height z . The Alfvén speed ν_a depends on the density of ions, which varies with altitude (and time of day). However, as we have pointed out, we are concerned only with the transmission properties of the lower ionosphere (i.e., below about 350 km). Over this region the ion density is relatively constant (except at the very bottom, where we will replace the very rapid actual variation with a discontinuity). We will assume that the Alfvén speed is constant throughout the whole ionosphere, with a value appropriate to the lower ionosphere. As we have stated previously, this approximation should have little effect on the calculated properties of the lower ionosphere. The same remarks apply to the ion cyclotron frequency ω_i , which is also assumed to be constant.

It now remains to approximate the ion-neutral particle collision frequency, ν_i . For reasons discussed above, it is sufficient to have an analytic approximation which is accurate only over the transition region. Over this region, the collision frequency is approximated rather well by an exponential; we therefore take ν_i to have the form

$$v_i = \omega_i e^{z/\zeta} \quad (23)$$

We have taken the plane $z = 0$ to be at that altitude at which $v_i = \omega_i$, or in other words, at the "boundary" between the Alfvén and transition regions, which occurs at an altitude of about 130 km. (The positive z -direction has been taken vertically downward, as before.) For the time being, the collision frequency scale-height ζ will be left as a parameter, with an appropriate numerical value to be assigned later. This will enable us to examine the role played by the transition region in determining the transmission coefficient.

It is convenient at this point to work with dimensionless quantities, which we shall denote by a tilde. To do so, we introduce the following units:

$$\begin{aligned} \text{unit of frequency} &= \omega_i \\ \text{unit of length} &= \frac{v_a}{\omega_i} \end{aligned}$$

In these units, the frequency range of interest is $\tilde{\omega} \ll 1$. Introducing these units and combining Eqs. (19), (20), and (23), we obtain

$$\frac{d^2 E}{dz^2} + f(\tilde{\omega}; \tilde{z}/\tilde{\zeta}) E = 0 \quad (24)$$

where

$$f(\tilde{\omega}; \tilde{z}/\tilde{\zeta}) = \frac{\tilde{\omega} - i\tilde{\omega}^2 e^{-\tilde{z}/\tilde{\zeta}}}{1 - i e^{-\tilde{z}/\tilde{\zeta}}} \quad (25)$$

The propagation problem actually extends down to the surface of the earth, which we treat as a perfect conductor at the low frequencies of interest to us. At the base of the ionosphere, the variation in composition is very rapid compared with the wavelength in its vicinity; we therefore replace the actual variation in composition by a discontinuity at $z = z_1$. With our choice of coordinate axes, the atmosphere is therefore divided in the following way into two

atmospheric regions (the upper of which we have already subdivided into ionospheric regions);

- $z < z_1$; ionosphere
- $(z = 0)$; altitude at which $v_1 = \omega_1$
- $z = z_1$; discontinuous transition to neutral atmosphere
- $z_1 < z < z_1 + h$; neutral atmosphere
- $z = z_1 + h$; surface of the earth.

The quantity h is the height of the neutral atmosphere.

Since the earth is assumed to be a perfect conductor, the field at the surface of the earth must vanish. In the neutral atmosphere, the field must therefore have the form

$$E = A_0(\tilde{\omega}) \sin \tilde{k}_0 (\tilde{z} - \tilde{z}_1 - \tilde{h}) \quad (26)$$

$$(\tilde{z}_1 < \tilde{z} < \tilde{z}_1 + \tilde{h})$$

where $A_0(\tilde{\omega})$ is some unknown function of $\tilde{\omega}$. The boundary condition we impose at the base of the ionosphere is that the field and its derivative are continuous, or that

$$\left\{ \frac{1}{E} \frac{dE}{d\tilde{z}} \right\}_{\tilde{z}=\tilde{z}_1-} = \left\{ \frac{1}{E} \frac{dE}{d\tilde{z}} \right\}_{\tilde{z}=\tilde{z}_1+} = -\tilde{k}_0 \cot \tilde{k}_0 \tilde{h} \approx -\frac{1}{\tilde{h}} \quad (27)$$

where the approximation of the cot follows from the fact that the wavelength in air is extremely long.

We next turn our attention to the solution of the wave equation in the ionosphere. From Eq. (25) it is apparent that for $\tilde{z}/\tilde{\zeta} \gg 1$ (i.e., in the Hall region), $f(\tilde{\omega}; \tilde{z}/\tilde{\zeta}) \approx \tilde{\omega}$. There must consequently exist two linearly independent solutions, W_1 and W_2 , cf Eq. (24) such that

$$W_1 \rightarrow e^{i\tilde{\omega}^{\frac{1}{2}} \tilde{z}}$$

$$W_2 \rightarrow e^{-i\tilde{\omega}^{\frac{1}{2}} \tilde{z}} \quad \tilde{z} \rightarrow \infty \quad (28)$$

We take our general solution of Eq. (24) to have the form

$$E = A_i(\tilde{\omega})(W_1 + \alpha W_2) \quad (29)$$

where $A_i(\tilde{\omega})$ and α are two, as yet unknown, functions of $\tilde{\omega}$. Since the asymptotic form given by Eq. (28) is a good approximation in the Hall region, we have

$$E \approx A_i(\tilde{\omega}) (e^{i\tilde{\omega}^{\frac{1}{2}} \tilde{z}} + \alpha e^{-i\tilde{\omega}^{\frac{1}{2}} \tilde{z}}) \quad (30)$$

$$(\tilde{z} \rightarrow \tilde{z}_1).$$

Using Eq. (30) to evaluate the left-hand side of Eq. (27) and solving for α , we obtain

$$\alpha = -e^{2i\tilde{\omega}^{\frac{1}{2}} \tilde{z}_1} \frac{(1 + i\tilde{\omega}^{\frac{1}{2}} \tilde{h})}{(1 - i\tilde{\omega}^{\frac{1}{2}} \tilde{h})}, \quad (31)$$

which, substituted back into Eq. (30) gives, for the electric field at the base of the ionosphere,

$$E(\tilde{z}_1; \tilde{\omega}) = A_i(\tilde{\omega}) \frac{(-2 i\tilde{\omega}^{\frac{1}{2}} \tilde{h})}{(1 - i\tilde{\omega}^{\frac{1}{2}} \tilde{h})} e^{i\tilde{\omega}^{\frac{1}{2}} \tilde{z}_1}. \quad (32)$$

To obtain a transmission and reflection coefficient, we must examine our solution, Eq. (30), in the Alfvén region ($\tilde{z}/\zeta \ll -1$). In the Alfvén region, Eq. (25) becomes $f(\tilde{\omega}; \tilde{z}/\zeta) \approx \tilde{\omega}^2$; consequently, any solution of Eq. (24) becomes some linear combination, in the Alfvén region, of the two linearly independent solutions $e^{i\tilde{\omega} \tilde{z}}$ and $e^{-i\tilde{\omega} \tilde{z}}$. We may therefore write

$$W_1 \rightarrow a_1 e^{i\tilde{\omega} \tilde{z}} + b_1 e^{-i\tilde{\omega} \tilde{z}}$$

$$W_2 \rightarrow a_2 e^{i\tilde{\omega} \tilde{z}} + b_2 e^{-i\tilde{\omega} \tilde{z}} \quad (33)$$

$$(\tilde{z} \rightarrow -\infty).$$

Combining Eqs. (33) and (29), we obtain for the field in the Alfvén region

$$E \approx A_1(\omega) (a_1 + \alpha a_2) (e^{i\tilde{\omega} \tilde{z}} + r e^{-i\tilde{\omega} \tilde{z}}), \quad (34)$$

$$(\tilde{z} \rightarrow -\infty)$$

where

$$r = \frac{b_1 + \alpha b_2}{a_1 + \alpha a_2}. \quad (35)$$

We shall refer to $|r|$ as the amplitude reflection coefficient; the square of this coefficient is the usual energy reflection coefficient.

From Eqs. (30) and (34), we can calculate the ratio of the electric field at the base of the ionosphere to the incoming-wave part of the electric field in the Alfvén region. This quantity, which we call the amplitude transmission coefficient for the electric field, and which we denote by t_E , is given by

$$t_E = \frac{E(\tilde{z}_1, \omega)}{A_1(\omega) (a_1 + \alpha a_2)} = - \frac{2i\tilde{\omega}^{\frac{1}{2}} \tilde{h} e^{i\tilde{\omega}^{\frac{1}{2}} \tilde{z}_1}}{(1 - i\tilde{\omega}^{\frac{1}{2}} \tilde{h}) (a_1 + \alpha a_2)}. \quad (36)$$

In practice, we are interested in the magnetic field at the surface of the earth which, at these extremely large wavelengths in air, is essentially the same as the magnetic field at the base of the ionosphere. Combining the induction equation with Eq. (27), we obtain

$$B(\tilde{z}_1, \omega) = \frac{1}{\tilde{\omega}} \left\{ \frac{dE}{d\tilde{z}} \right\}_{\tilde{z} = \tilde{z}_1} = - \frac{c}{\omega \tilde{h}} E(\tilde{z}_1, \omega), \quad (37)$$

where $B = B_x - i B_y$. On the other hand, the induction equation applied to Eq. (34) gives

$$B \approx i\tilde{c}A_1(\tilde{\omega})(a_1 + \alpha a_2)(e^{i\tilde{\omega}\tilde{z}} - r e^{-i\tilde{\omega}\tilde{z}}),$$

$$(\tilde{z} \rightarrow -\infty)$$

so that, in analogy with Eq. (36), the amplitude transmission coefficient for the magnetic field, which we denote by t_B , is given by

$$t_B = \frac{B(\tilde{z}_1, \tilde{\omega})}{\tilde{c}A_1(\tilde{\omega})(a_1 + \alpha a_2)} = \frac{2 e^{i\tilde{\omega}^{\frac{1}{2}} \tilde{z}_1}}{\tilde{\omega}^{\frac{1}{2}}(1 - i\tilde{\omega}^{\frac{1}{2}} \tilde{h})(a_1 + \alpha a_2)}. \quad (38)$$

It remains now only to determine the quantities a_1 , a_2 , b_1 , and b_2 . These are obtained by determining the solutions, W_1 and W_2 , of Eq. (24) which have the form prescribed by Eq. (28) and examining them in the limit $\tilde{z} \rightarrow -\infty$, where they must assume the form given by Eq. (33). In order to avoid introducing any unnecessary mathematical detail at this point, we shall defer this procedure to the Appendix and merely present the results in the next section.

V. TRANSMISSION AND REFLECTION COEFFICIENTS

The numerical results presented in this section will be based on the following values of the relevant parameters, chosen to coincide with the ionosphere of Francis and Karplus (1960):

$$h = 80 \text{ km}$$

$$z_1 = 50 \text{ km}$$

$$\omega_i \text{ (unit of frequency)} = 175 \text{ rad/sec}$$

$$\frac{v_a}{\omega_i} \text{ (unit of length)} = \frac{1.2}{N_i^{1/2}} \text{ km}$$

$$N_i = \text{ion density in (no./cc)} \times 10^{-6}.$$

We recall that the cyclotron frequency ω_i is considered constant throughout the ionosphere; the numerical value chosen for ω_i is that frequency at which $v_i = \omega_i$ in the actual ionosphere, which, by Eq. (20), also defines the plane $z = 0$. The numeric in the unit of length is based on an ion atomic weight of 26, which is also appropriate to the region around $z = 0$, i.e., around 130 km.

To obtain the transmission and reflection coefficients, we must introduce the expressions obtained in the Appendix for a_1 , a_2 , b_1 , and b_2 into Eqs. (38) and (35). The results are most conveniently expressed in terms of a function $g(\tilde{\omega}^{1/2}, \tilde{\omega})$ defined by

$$g(\tilde{\omega}^{1/2}, \tilde{\omega}) = \frac{\Gamma(1 - 2i\zeta \tilde{\omega}^{1/2})}{2 [\Gamma(1 - i\zeta \tilde{\omega}^{1/2} - i\zeta \tilde{\omega})]} (1 - i\tilde{\omega}^{1/2} \tilde{\omega}) \exp(\frac{\pi}{2} \zeta \tilde{\omega}^{1/2} - \frac{\pi}{2} \zeta \tilde{\omega} - i\tilde{z}_1 \tilde{\omega}^{1/2}) \quad (39)$$

where, as usual, Γ denotes the Gamma-function. Combining the results of the Appendix with Eqs. (35) and (38), respectively, we obtain

$$r = - \frac{(1 - \tilde{\omega}^{1/2}) g(\tilde{\omega}^{1/2}, -\tilde{\omega}) + (1 + \tilde{\omega}^{1/2}) g(-\tilde{\omega}^{1/2}, -\tilde{\omega})}{(1 + \tilde{\omega}^{1/2}) g(\tilde{\omega}^{1/2}, \tilde{\omega}) + (1 - \tilde{\omega}^{1/2}) g(-\tilde{\omega}^{1/2}, \tilde{\omega})} \quad (40)$$

and

$$t_B = \frac{4}{\Gamma(1 - 2i\zeta\tilde{\omega})[(1 + \tilde{\omega}^{\frac{1}{2}})g(\tilde{\omega}^{\frac{1}{2}}, \tilde{\omega}) + (1 - \tilde{\omega}^{\frac{1}{2}})g(-\tilde{\omega}^{\frac{1}{2}}, \tilde{\omega})]} \quad (41)$$

(As far as the functional form of g is concerned, $\tilde{\omega}^{\frac{1}{2}}$ and $\tilde{\omega}$ are treated as independent.)

Before obtaining numerical results for r and t_B , it will be instructive to examine the limiting case $\zeta = 0$. As can be seen from Eq. '23), this case corresponds to a collision frequency

$$\begin{aligned} v_i &= 0 & z < 0 \\ v_i &= \infty & z > 0, \end{aligned} \quad (42)$$

and therefore to a medium consisting of two uniform layers, an Alfvén region and a Hall region, (in which, despite the infinite collision frequency, it is still assumed that the neutral particles do not participate in the mass motion), separated by a sharp boundary at $z = 0$. (This limiting case can, of course, be obtained much more simply by direct calculation.) With $\zeta = 0$, all of the Gamma-functions in the above expressions are unity, and considerable simplification results. It is not difficult to show, for example, that

$$|r| = 1 \quad (43)$$

for both the L-mode and the R-mode, although the physical significance of this result is quite different for the two modes. For the L-mode, this is an expression of the fact that both regions are lossless (real index of refraction in both regions), and the perfectly conducting earth reflects all of the incident energy. On the other hand, the R-mode, as we have pointed out previously, has a pure imaginary index of refraction in the Hall region, and is consequently evanescent in this region. This, coupled with the boundary

condition which we have imposed at the surface of the earth, makes this evanescent region look infinite to the incoming wave (although with an index of refraction somewhat different from that of the actual Hall region), and consequently leads to total reflection.

The transmission coefficient, in this limiting case, is given by

$$t_B = \frac{4}{[(1 + \tilde{\omega}^{\frac{1}{2}})(1 - i\tilde{\omega}^{\frac{1}{2}}\tilde{h}) e^{-i\tilde{z}_1\tilde{\omega}^{\frac{1}{2}}} + (1 - \tilde{\omega}^{\frac{1}{2}})(1 + i\tilde{\omega}^{\frac{1}{2}}\tilde{h}) e^{i\tilde{z}_1\tilde{\omega}^{\frac{1}{2}}}]}. \quad (44)$$

This coefficient will exhibit resonances at frequencies for which the denominator of Eq. (44) becomes small. It is a well-known result that the nature of such resonances is intimately related to the location in the complex $\tilde{\omega}$ -plane of the poles of the transmission coefficient. If a pole lies close to the real $\tilde{\omega}$ -axis (and we shall show shortly that this is indeed the case for the poles of Eq. (44) in the frequency range of interest) it represents a resonance, the real part of the pole giving the position of the resonance and the imaginary part giving its width.

Now, the poles of Eq. (44) are the roots of the equation

$$(1 + \tilde{\omega}^{\frac{1}{2}})(1 - \tilde{\omega}^{\frac{1}{2}}\tilde{h}) e^{-i\tilde{z}_1\tilde{\omega}^{\frac{1}{2}}} + (1 - \tilde{\omega}^{\frac{1}{2}})(1 + i\tilde{\omega}^{\frac{1}{2}}\tilde{h}) e^{i\tilde{z}_1\tilde{\omega}^{\frac{1}{2}}} = 0. \quad (45)$$

We are interested in the frequency range $\tilde{\omega}^{\frac{1}{2}} \ll 1$, where Eq. (45) becomes, approximately,

$$\cot(\tilde{\omega}^{\frac{1}{2}}\tilde{z}_1) - \tilde{\omega}^{\frac{1}{2}}\tilde{h} = 0. \quad (46)$$

It is not difficult to show that the roots, $\tilde{\omega}_n$, of this approximate equation are pure real and, consequently, that the low-frequency

poles of Eq. (44) lie very close to the real ω -axis, as was stated above. These poles thus represent very sharp resonances, as can be seen in Fig. 1 where $|t_B|$, for the L-mode, is plotted against $\tilde{\omega}$ for the case $\zeta = 0$ (with $z_1 = 50$ km and $h = 80$ km), for ion densities of $5 \times 10^5/\text{cc}$, $10^5/\text{cc}$, and $5 \times 10^3/\text{cc}$. The three values chosen for the ion density are representative, in order of increasing density, of conditions in the daytime at sunspot maximum, in the daytime at sunspot minimum, and in the nighttime, respectively.

A simple physical interpretation of these resonances exists in the limiting case where we ground the ionosphere at its base, i.e., for the case $h = 0$. In this case, the roots of Eq. (46) are given by

$$\tilde{\omega}_n^{\frac{1}{2}} \tilde{z}_1 = \frac{2\pi}{\tilde{\lambda}_n} \tilde{z}_1 = (2n-1) \frac{\pi}{2},$$

$$n = 1, 2, \dots \quad (47)$$

where $\tilde{\lambda}_n$ is the wavelength in the Hall region. The lowest root therefore corresponds to the frequency at which the Hall region is a quarter-wave plate. However, it should be noted that, since the term $\tilde{\omega}^{\frac{1}{2}} \tilde{h}$ in Eq. (46) is of order unity even for the lowest of these roots, the inclusion of a neutral atmosphere between the base of the ionosphere and ground plays a very important role in determining the positions of the resonant frequencies. For example, for the case of an ion density of $5 \times 10^5/\text{cc}$, the lowest frequency determined by Eq. (47) is $\tilde{\omega}_0 = 3 \times 10^{-3}$, whereas the lowest root of Eq. (46) is actually at $\tilde{\omega} = 6 \times 10^{-4}$, a factor of 5 lower. Thus, the resonances are shifted toward significantly lower frequencies by the inclusion of a region of neutral atmosphere. This emphasizes the importance of including such a region in any calculation of ionospheric transmission coefficients.

Before leaving this two-layer limit, we note from Fig. 1 that the transmission resonances show an upward shift in frequency from day to night, and from sunspot maximum to sunspot minimum, as is observed for Pc oscillations. This result persists even when a transition region is introduced. This is best understood by rewriting Eq.

(46) in terms of the dimensional lengths z_i and h , recalling that the unit of length is $v_a/\omega_i = c_i N_i^{-1/2}$, where c_i is a constant which depends only on the ion mass. In terms of these quantities, Eq. (46) becomes

$$\cot(\tilde{\omega}^{1/2} N_i^{1/2} c_i z_i) - \tilde{\omega}^{1/2} N_i^{1/2} c_i h = 0. \quad (48)$$

It is clear that the roots of this equation can be written

$$\tilde{\omega}_n^{1/2} N_i^{1/2} = d_n \quad (49)$$

where the d_n are constants independent of ionospheric conditions. We thus find that each resonant frequency varies inversely with ion density. This result holds strictly in the two-layer limit only for $\tilde{\omega}^{1/2} \ll 1$, since Eq. (46) was derived from Eq. (45) on the basis of that assumption. With the same limitation on $\tilde{\omega}$, this same result can be shown to apply in the general case to the roots of Eq. (41), as well.

The two-layer limit considered above has two major inadequacies: it introduces an artificial sharp boundary between the Alfvén and Hall regions, which may give rise to spurious resonances, and it fails to include the effects of collisional losses, the very region in which such losses occur having been eliminated in this limit. To include a transition region, we must calculate the transmission and reflection coefficients for an appropriate value of the scale height, ζ . There seems to be considerable disagreement, however, as to what the appropriate ionospheric scale height is. From the ionosphere of Francis and Karplus (1960), for example, a scale height of 14 km would appear appropriate, whereas the ionosphere of Prince and Bostick (1964) puts the scale height closer to 10 km. Because of this uncertainty in the best value of ζ , we shall present the results for both $\zeta = 10$ km and $\zeta = 14$ km. This will, at the same time, enable us to study the role of the transition region in the determination of the transmission and reflection coefficients.

In Figs. 2 and 3, we have plotted $|t_B|$, for the L-mode, for scale heights of $\zeta = 10$ km and $\zeta = 14$ km, respectively, for different values of the ion density. (The Gamma-functions of complex argument were calculated on an IBM 7044 electronic computer.) A comparison of these figures with Fig. 1 for the layered medium shows that the most striking effect of the inclusion of a transition region is the virtual elimination of all but the lowest resonance, which is in turn considerably depressed and broadened compared to the layered case. This qualitative change in transmission characteristics results primarily from the removal of the artificial sharp boundary of the two-layer limit. The lowest resonance still remains, because at this frequency the wavelength is many times the scale height of the transition region, so that the transition from Alfvén to Hall region appears relatively sharp. At the higher frequencies, however, the wavelength is comparable with or smaller than the scale height, so that one region appears to change slowly and continuously into the other.

The effects of losses in the transition region are contained mainly in the reflection coefficient, since, with our model of a perfectly reflecting earth, all the energy which is not reflected is absorbed. In Figs. 4 and 5, we have plotted $|r|$, for the L-mode, for three different densities. (We recall that $|r|^2$ is the energy reflection coefficient.) A comparison of these figures with Figs. 2 and 3 shows that absorption becomes important, for a given ion density, at frequencies somewhat higher than the corresponding lowest resonance. It is also apparent that the reflection coefficient exhibits characteristic minima in the neighborhood of the maxima of the corresponding transmission coefficient. These minima, which represent absorption maxima, become more pronounced at higher frequencies.

A comparison of Figs. 2 and 3 with Fig. 1 shows that the introduction of a transition region shifts the resonances, but not drastically, to somewhat lower frequencies. These resonances are thus essentially still those frequencies at which the Hall region becomes transparent. The downward shift produced by the inclusion of a transition region results from the fact that such a region increases the effective size of the Hall region.

Based on a value of $\omega_i = 175$ rad/sec, the lowest resonances occur at a frequency of .014 cps for $\zeta = 10$ km and at a frequency of .013 cps for $\zeta = 14$ km. The agreement with the 70 second period observed by Maple (1959) is undoubtedly fortuitous, but the general location of these resonances makes it seem very probable that they are responsible for Pc oscillations. Another point in support of this suggestion is the fact that these resonances, besides being shifted to higher frequencies from day to night, are also considerably depressed at night. This would account for the fact that Pc oscillations are mainly a daytime phenomenon.

One further point worthy of note in connection with Figs. 2 and 3 is that the ionosphere becomes essentially transparent at night up to frequencies of the order of 1 cps. On the other hand, in the daytime the transmission coefficient becomes rather small for frequencies greater than about .05 cps. This would account for the fact that "pearl" type oscillations, which have frequencies of the order of .1 cps, are mostly a nighttime phenomenon. In the daytime, they are apparently filtered out by the Hall region.

In Figs. 6, 7, and 8, we have plotted $|t_B|$ for the R-mode, i.e., for $\tilde{\omega} < 0$. It is apparent that the transmission coefficient for this mode drops off very rapidly with frequency compared to that for the L-mode. At resonance, the transmitted wave is almost entirely of the L-type, and consequently left-circularly polarized, as mentioned previously.

In Figs. 9 and 10, we have plotted $|r|$ for the R-mode, again for three different ion densities. It can be seen that, for low frequencies, this mode is almost totally reflected, indicating that it is nearly evanescent at these low frequencies. For frequencies higher than about 1 cps, however, significant absorption begins to take place, especially at the higher ion densities.

Finally, we should mention that we have considered only the steady-state problem. The transmitted signal resulting from a given source, however, is determined not only by the transmission

coefficient, but also by the frequency spectrum of the source. For a given source spectrum, however, the resulting signal can be calculated from the transmission coefficient given by Eq. (40). This involves a Fourier integral over frequency of the transmission coefficient weighted with the source spectrum. The usual technique for evaluating such integrals is to transform them to contour integrals in the complex $\tilde{\omega}$ -plane. The integral then becomes the sum of the residues of the integrand at the poles of the transmission coefficient. A procedure for determining the poles of Eq. (40) in the complex $\tilde{\omega}$ -plane has been presented elsewhere (Greifinger and Greifinger, 1964). At this point we would only remark that any transmitted signal becomes the sum of a number of resonance-like terms, with coefficients depending on the source spectrum. The higher frequencies are damped out more rapidly than the lower ones, so that eventually the signal is almost purely sinusoidal, its frequency being given by the real part of the appropriate pole of the transmission coefficient. This is very nearly the value of $\tilde{\omega}$ at which the transmission coefficient has its maximum on the real $\tilde{\omega}$ -axis, i.e., at the resonant frequency calculated above.

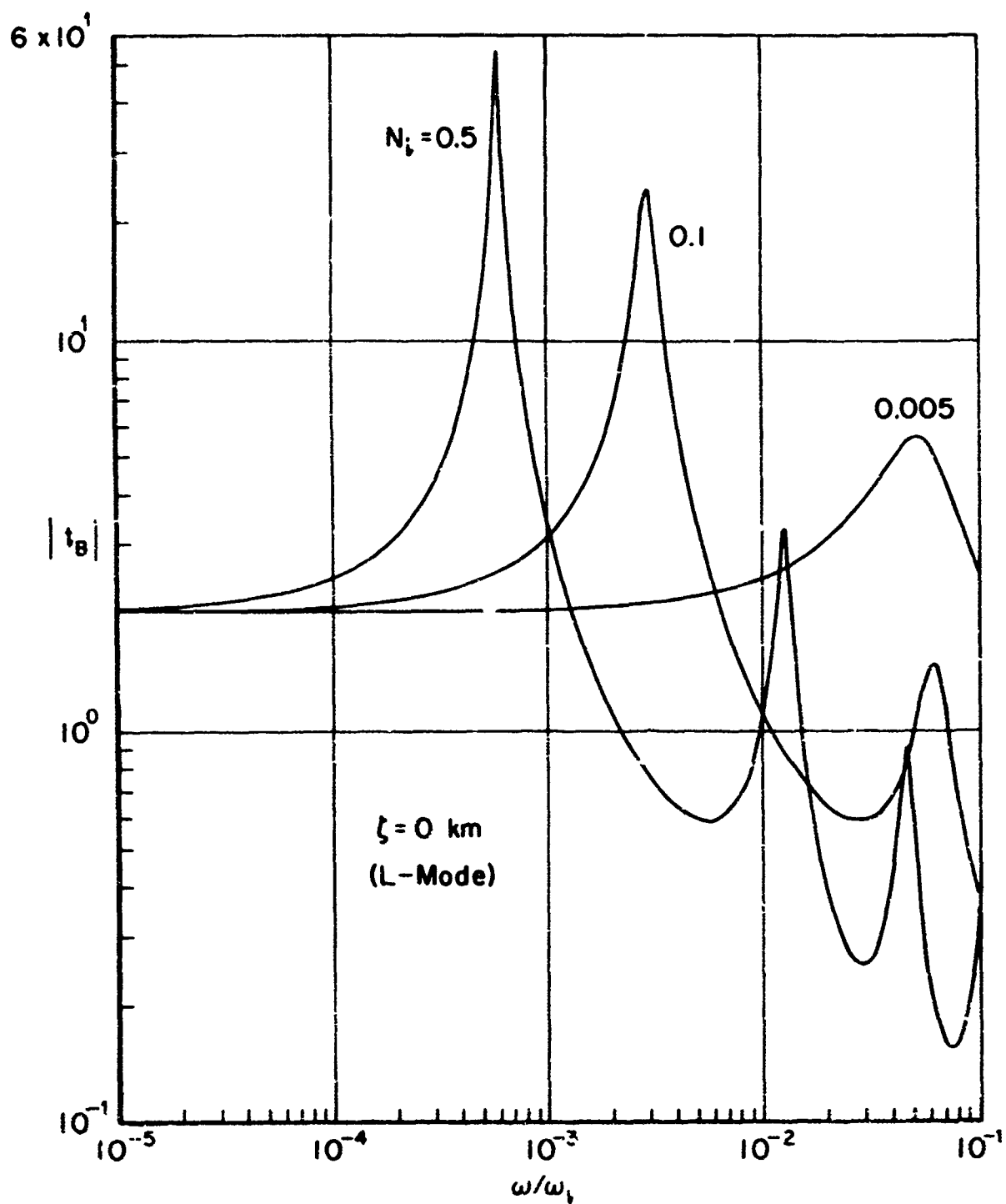


Fig. 1 - Amplitude of transmitted magnetic field, for unit amplitude of incident magnetic field, as a function of frequency, for different ionospheric conditions. (N_i is the ion number density in units of $10^6/\text{cc}$ and ω_i is the ion cyclotron frequency)

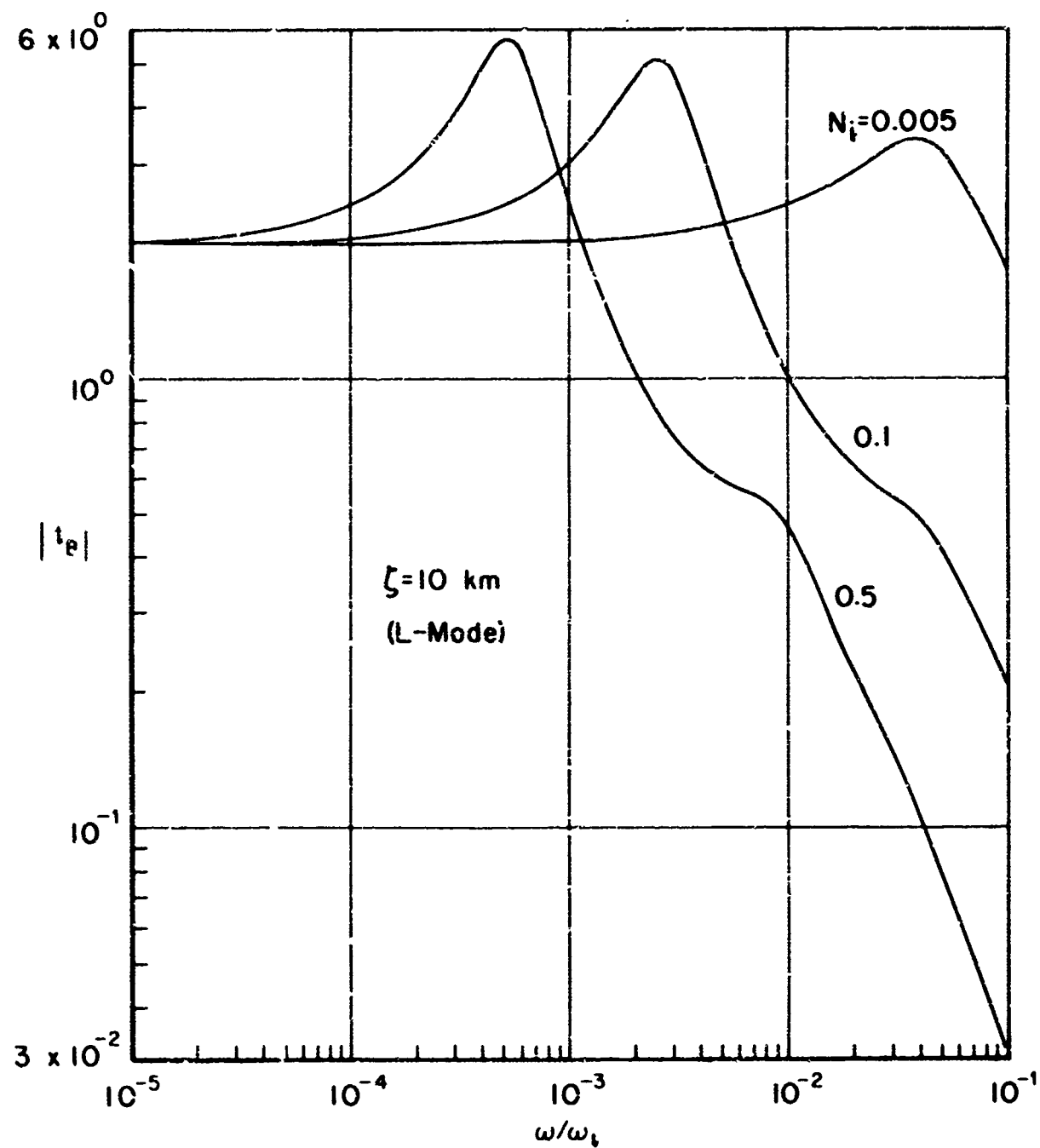


Fig. 2 - Amplitude of transmitted magnetic field, for unit amplitude of incident magnetic field, as a function of frequency, for different ionospheric conditions. (N_i is the ion number density in units of $10^6/\text{cc}$ and ω_i is the ion cyclotron frequency.)

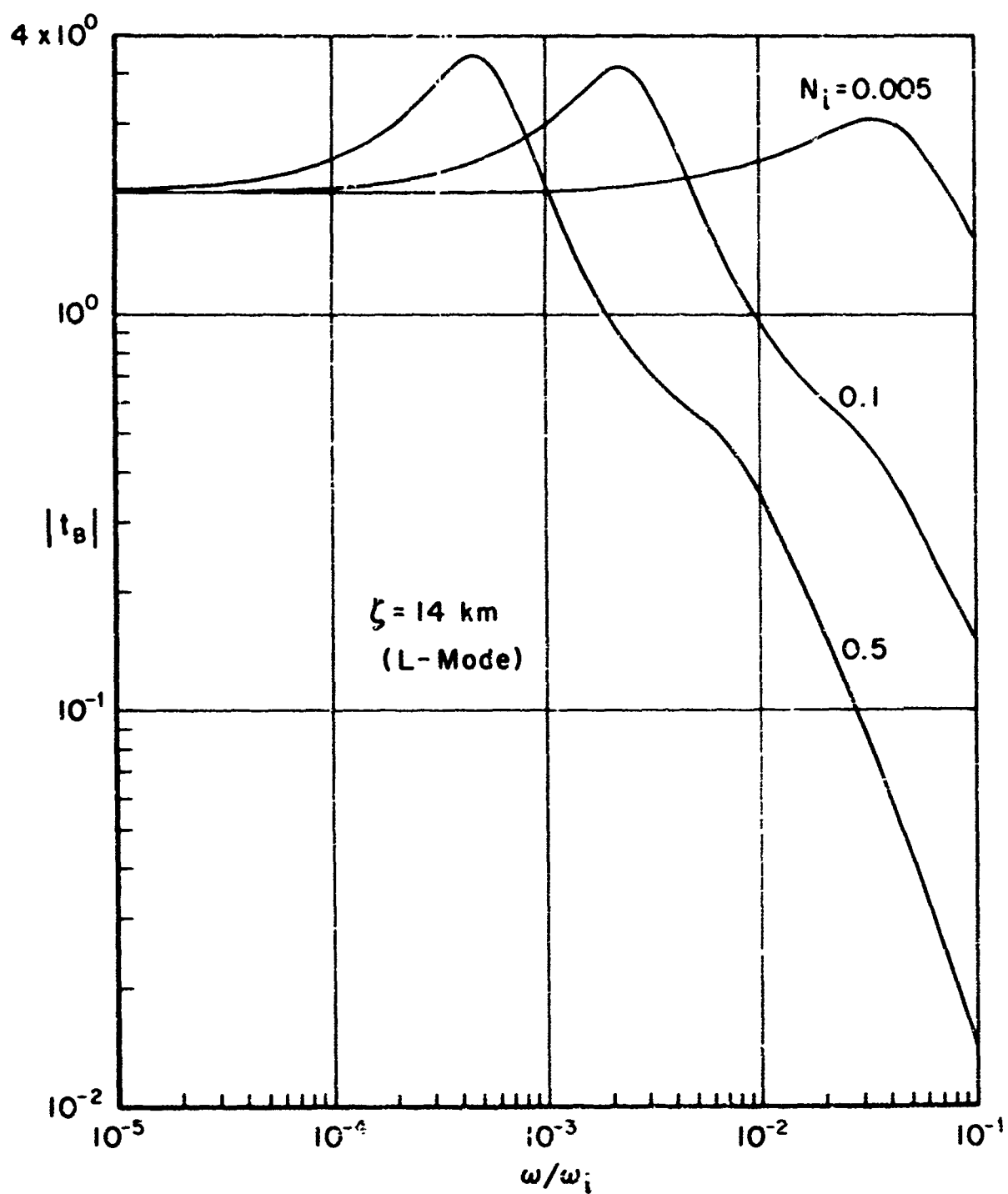


Fig. 3 -- Amplitude of transmitted magnetic field, for unit amplitude of incident magnetic field, as a function of frequency, for different ionospheric conditions. (N_i is the ion number density in units of $10^6/\text{cc}$ and ω_i is the ion cyclotron frequency.)

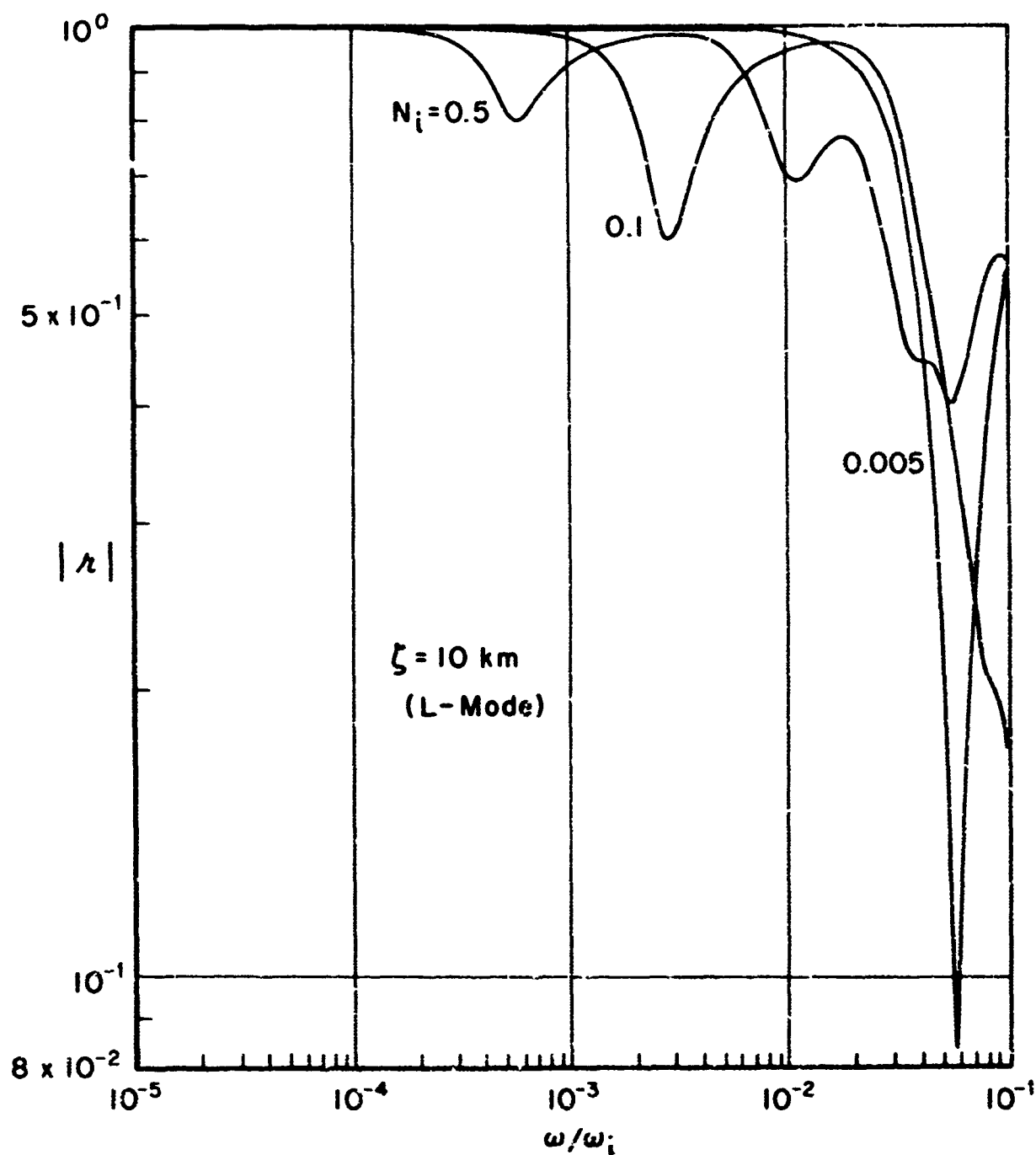


Fig. 4 - Amplitude of reflected magnetic (or electric) field, for unit amplitude of incident magnetic (or electric) field, as a function of frequency, for different ionospheric conditions. (N_i is the ion number density in units of $10^6/\text{cc}$ and ω_i is the ion cyclotron frequency)

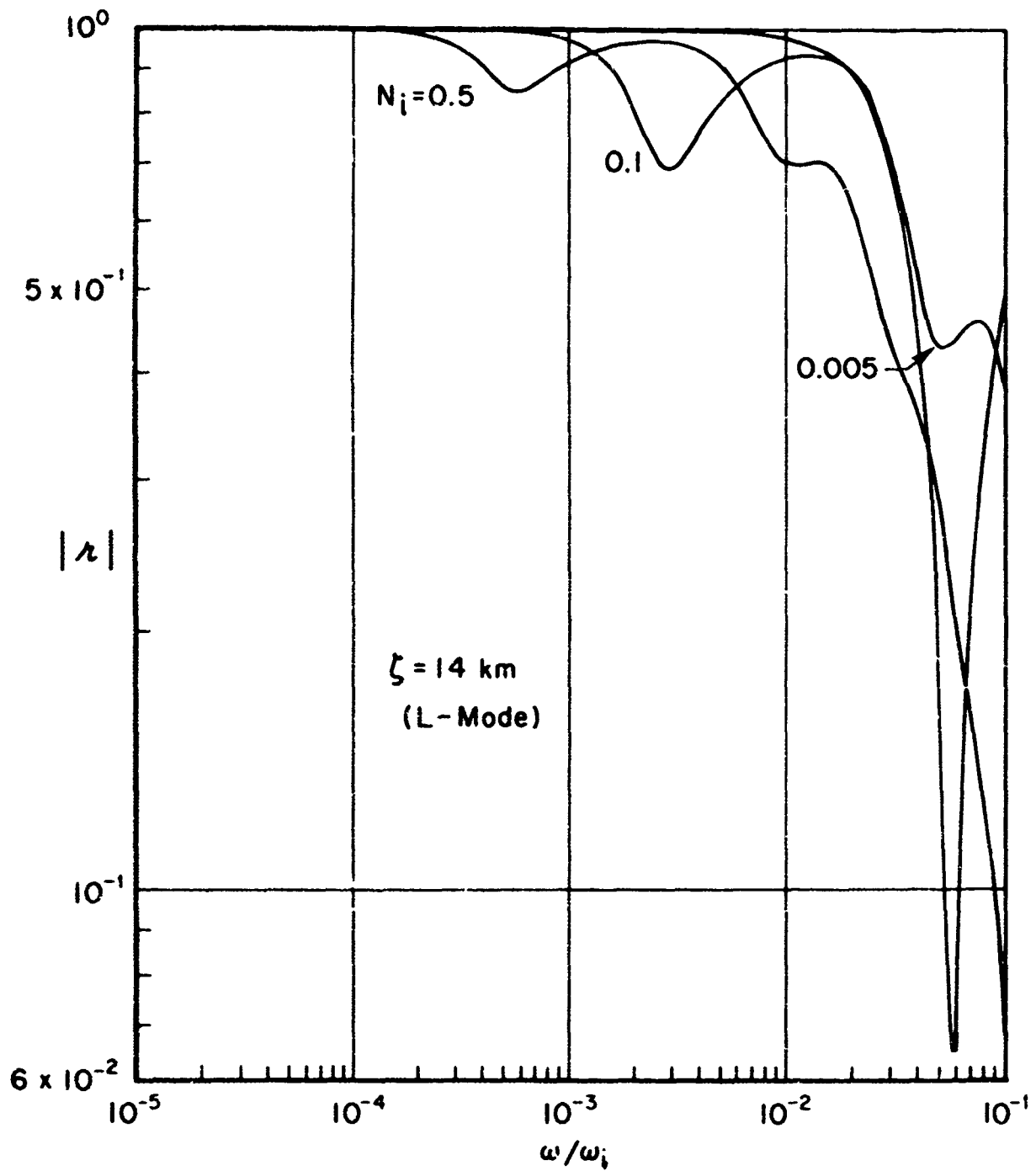


Fig. 5 - Amplitude of reflected magnetic (or electric) field, for unit amplitude of incident magnetic (or electric) field, as a function of frequency, for different ionospheric conditions. (N_i is the ion number density in units of $10^6/\text{cc}$ and ω_i is the ion cyclotron frequency.)

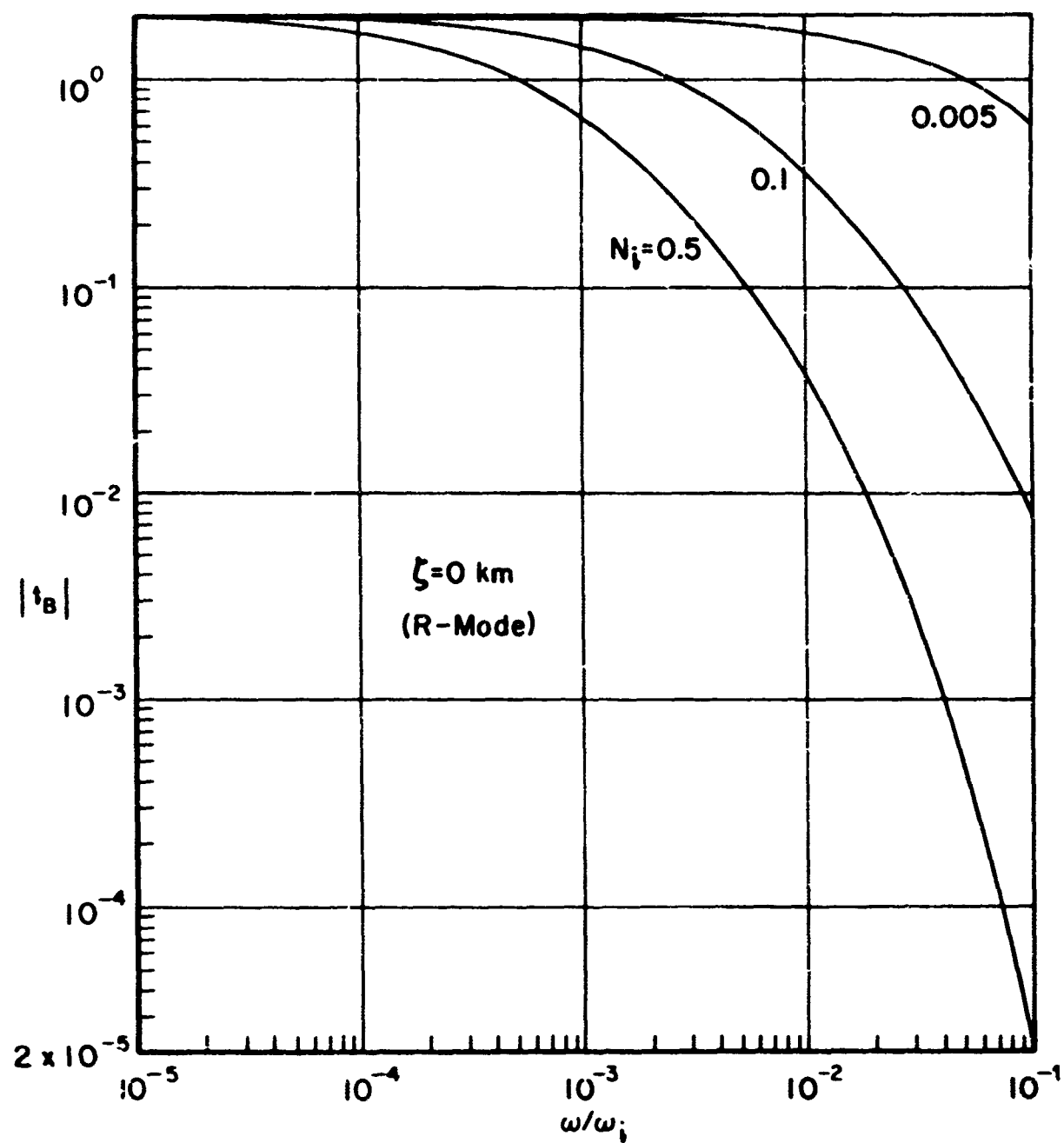


Fig. 6 - Amplitude of transmitted magnetic field, for unit amplitude of incident magnetic field, as a function of frequency, for different ionospheric conditions. (N_i is the ion number density in units of $10^6/\text{cc}$ and ω_i is the ion cyclotron frequency.)

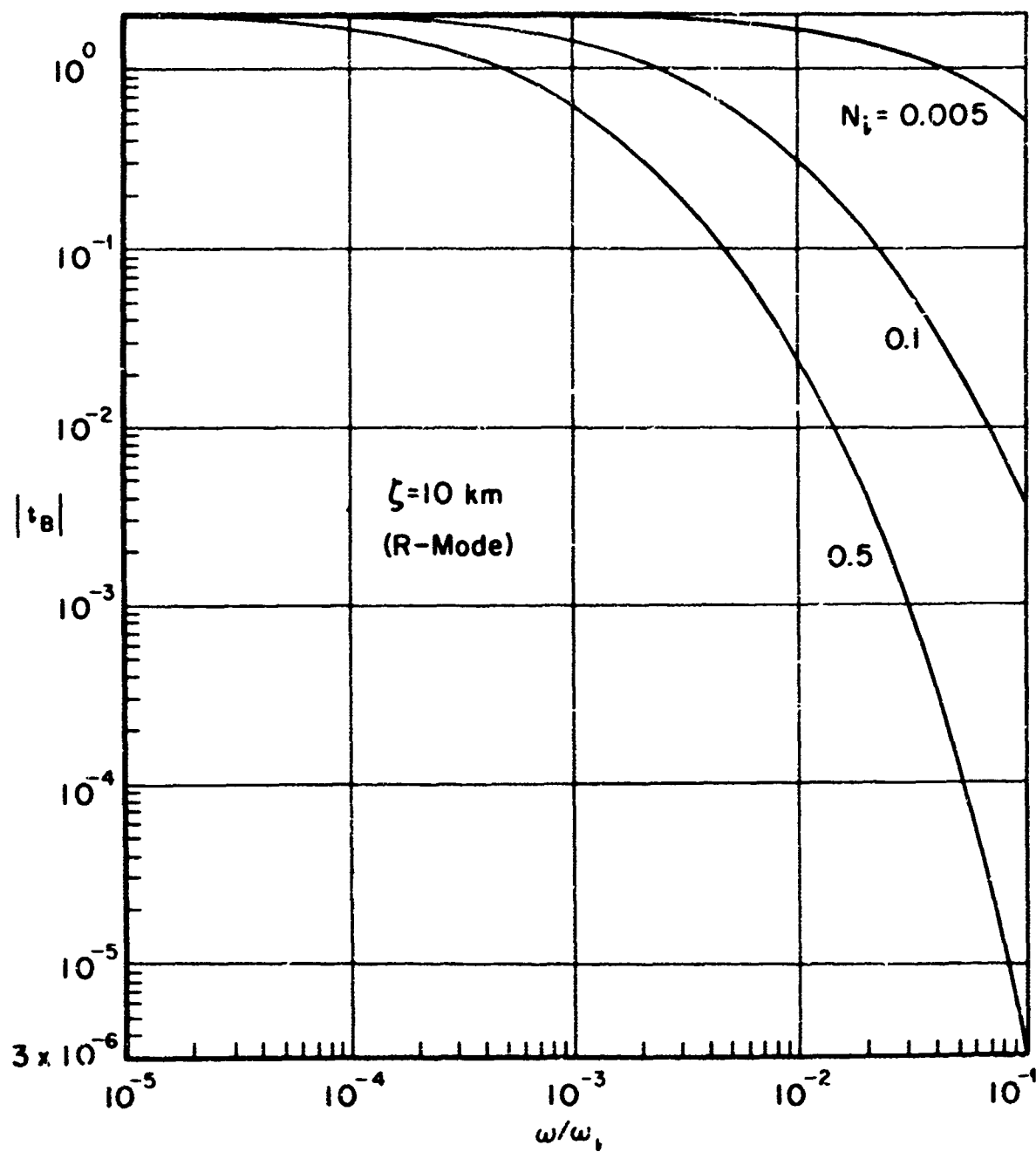


Fig. 7 - Amplitude of transmitted magnetic field, for unit amplitude of incident magnetic field, as a function of frequency, for different ionospheric conditions. (N_i is the ion number density in units of $10^6/\text{cc}$ and ω_i is the ion cyclotron frequency.)

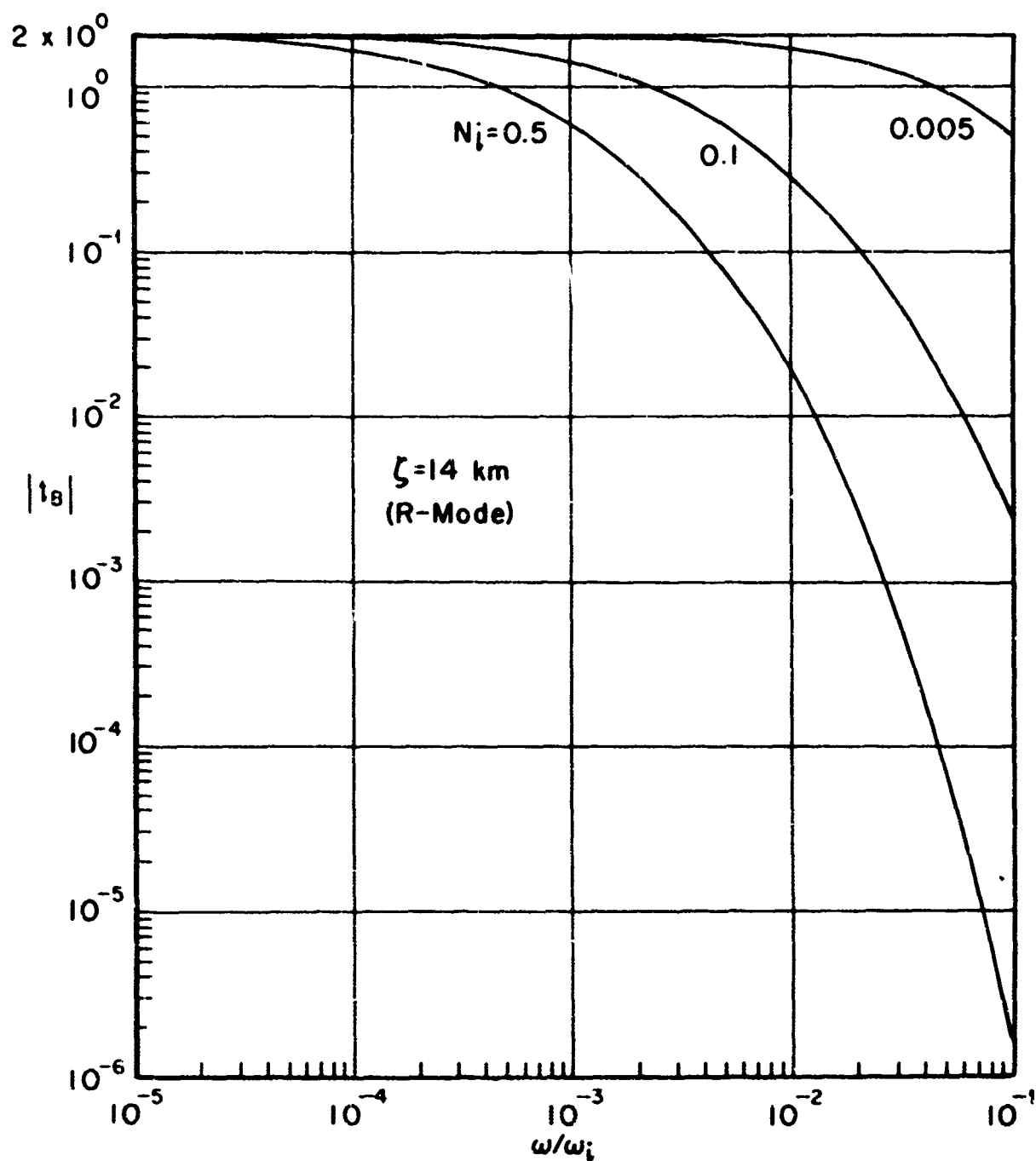


Fig. 8 - Amplitude of transmitted magnetic field, for unit amplitude of incident magnetic field, as a function of frequency, for different ionospheric conditions. (N_i is the ion number density, in units of $10^6/\text{cc}$ and ω_i is the ion cyclotron frequency.)

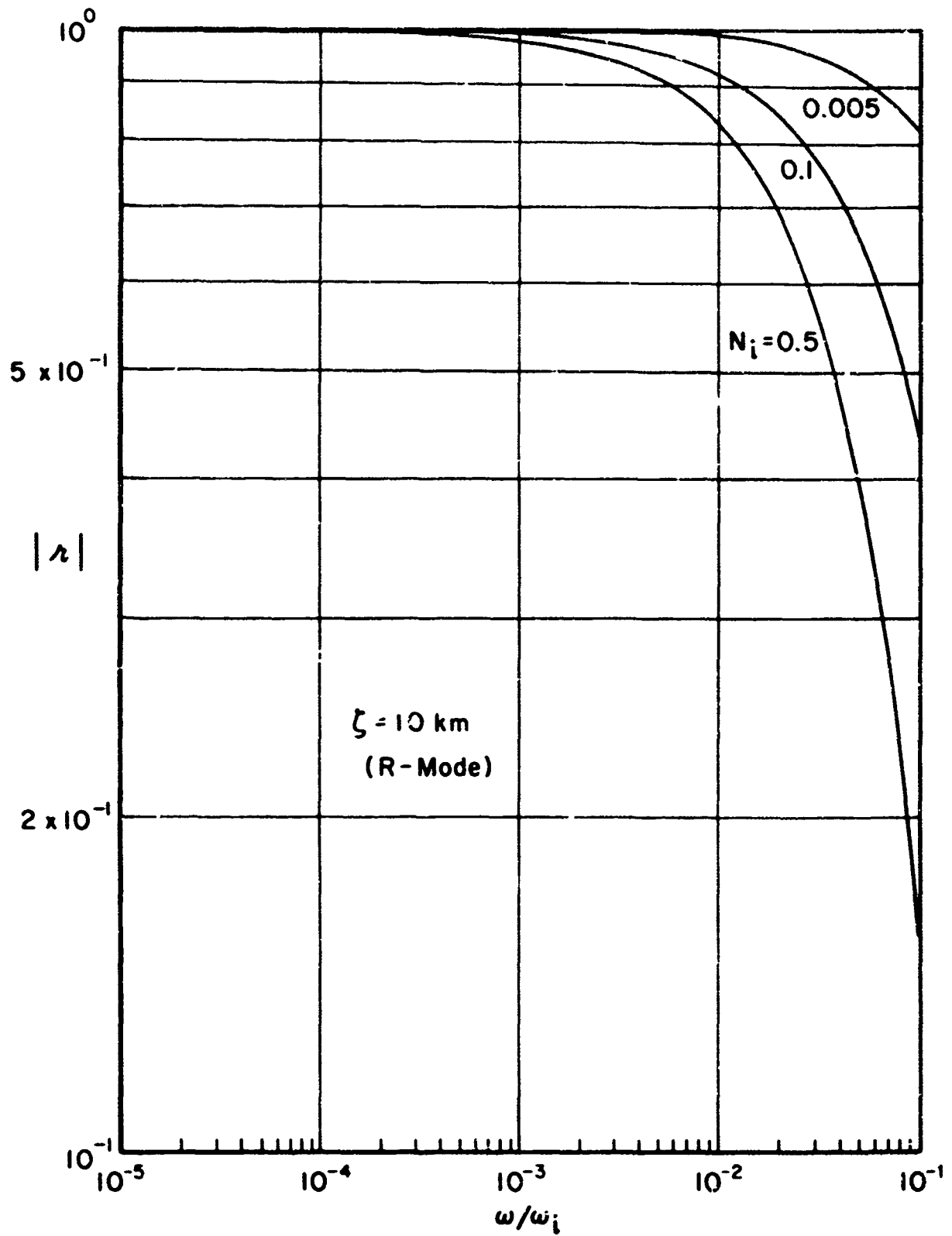


Fig. 9 - Amplitude of reflected magnetic (or electric) field, for unit amplitude of incident magnetic (or electric) field, as a function of frequency, for different ionospheric conditions. (N_i is the ion number density in units of $10^6/\text{cc}$ and ω_i is the ion cyclotron frequency.)

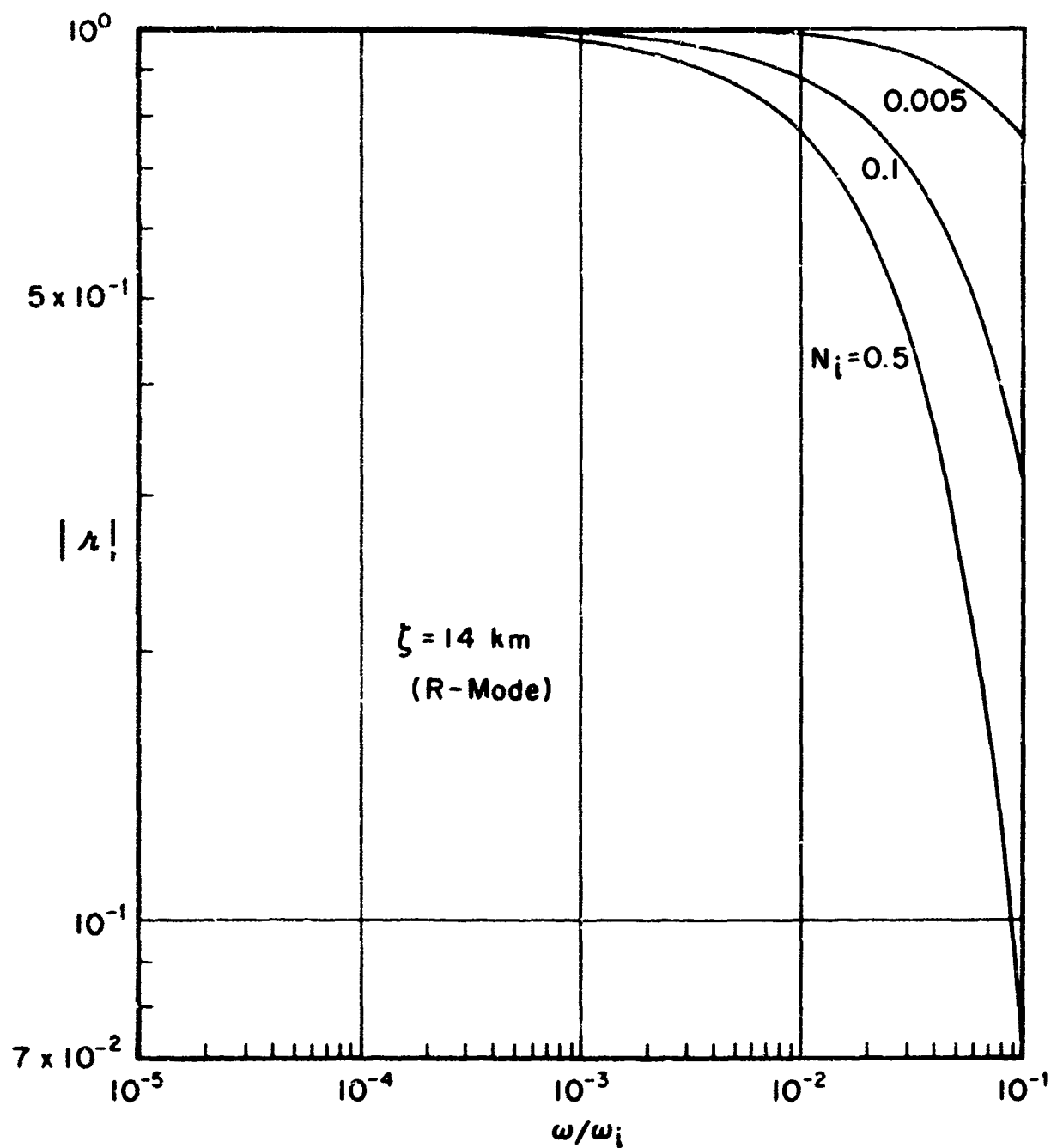


Fig. 10 - Amplitude of reflected magnetic (or electric) field, for unit amplitude of incident magnetic (or electric) field, as a function of frequency, for different ionospheric conditions. (N_i is the ion number density in units of $10^6/\text{cc}$ and ω_i is the ion cyclotron frequency.)

APPENDIX

In order to solve Eq. (24), we make the following change of variable:

$$u = 1 - i e^{-\tilde{z}/\zeta} = 1 + e^{-i\pi/2} e^{-\tilde{z}/\zeta}. \quad (A1)$$

In terms of this variable, Eq. (24) becomes

$$\frac{d^2 E}{du^2} + \frac{1}{u(u-1)} \frac{dE}{du} + \left[\frac{\tilde{\gamma}^2 \tilde{\omega}}{u(u-1)^2} + \frac{\tilde{\gamma}^2 \tilde{\omega}^2}{u(u-1)} \right] E = 0. \quad (A2)$$

This is to be compared with the canonical form of the hypergeometric equation

$$\frac{d^2 F}{du^2} + \left[\frac{\gamma + \gamma' - 1}{u} + \frac{\beta + \beta' - 1}{(u-1)} \right] \frac{dF}{du} + \left[\frac{\gamma\gamma'}{u} - \frac{\beta\beta'}{(u-1)} - \alpha\alpha' \right] \frac{1}{u(u-1)} F = 0. \quad (A3)$$

These equations become identical if we set

$$\begin{aligned} \alpha &= -\alpha' = i\tilde{\gamma}\tilde{\omega} \\ \beta &= -\beta' = i\tilde{\gamma}\tilde{\omega}^{\frac{1}{2}} \\ \gamma &= 0, \gamma' = 1. \end{aligned} \quad (A4)$$

We are looking for solutions of Eq. (A2) which have the form prescribed by Eq. (28), viz.,

$$\begin{aligned} W_1 &\rightarrow e^{i\tilde{\omega}^{\frac{1}{2}} \tilde{z}} \\ W_2 &\rightarrow e^{-i\tilde{\omega}^{\frac{1}{2}} \tilde{z}} \end{aligned} \quad (z \rightarrow \infty). \quad (A5)$$

In terms of the variable u defined by Eq. (A1), these solutions must have the form

$$\begin{aligned} W_1 &\rightarrow e^{\pi/2} \zeta \tilde{\omega}^{\frac{1}{2}} (u-1)^{-i\zeta \tilde{\omega}^{\frac{1}{2}}} \\ W_2 &\rightarrow e^{-\pi/2} \zeta \tilde{\omega}^{\frac{1}{2}} (u-1)^{i\zeta \tilde{\omega}^{\frac{1}{2}}} \end{aligned} \quad (u \rightarrow 1). \quad (A6)$$

The solutions of Eq. (A2) which have the form required by Eq. (A6) are

$$\begin{aligned} W_1 &= e^{\frac{\pi}{2} \zeta \tilde{\omega}^{\frac{1}{2}}} (u-1)^{-i\zeta \tilde{\omega}^{\frac{1}{2}}} F(-i\zeta \tilde{\omega} + i\zeta \tilde{\omega}, -i\zeta \tilde{\omega}^{\frac{1}{2}} - i\zeta \tilde{\omega}; \\ &\quad 1 - 2i\zeta \tilde{\omega}^{\frac{1}{2}}; - (u-1)) \\ W_2 &= e^{-\frac{\pi}{2} \zeta \tilde{\omega}^{\frac{1}{2}}} (u-1)^{i\zeta \tilde{\omega}^{\frac{1}{2}}} F(i\zeta \tilde{\omega}^{\frac{1}{2}} + i\zeta \tilde{\omega}, i\zeta \tilde{\omega}^{\frac{1}{2}} - i\zeta \tilde{\omega}; \\ &\quad 1 + 2i\zeta \tilde{\omega}^{\frac{1}{2}}; - (u-1)), \end{aligned} \quad (A7)$$

where F is the usual hypergeometric function.

We now need to evaluate W_1 and W_2 in the limit $z \rightarrow -\infty$, which, from Eq. (A1), is the limit $u \rightarrow \infty$. To do this, we make use of the analytic continuation which relates the hypergeometric function of argument x and the hypergeometric function of argument x^{-1} , viz.,

$$\begin{aligned} \frac{\Gamma(a)\Gamma(b)}{\Gamma(c)} F(a, b; c; x) &= \frac{\Gamma(a)\Gamma(b-a)}{\Gamma(c-a)} (-x)^{-a} F(a, 1-c+a; 1-b+a; x^{-1}) \\ &+ \frac{\Gamma(b)\Gamma(a-b)}{\Gamma(c-b)} (-x)^{-b} F(b, 1-c+b; 1-a+b; x^{-1}) \\ &| \arg(-x) | < \pi, \end{aligned} \quad (A8)$$

where Γ is the usual Γ -function. We apply Eq. (A8) to Eq. (A7) and take the limit $u \rightarrow \infty$, where the hypergeometric functions may be replaced by unity. It is then easy to show that Eq. (A7) becomes

$$\begin{aligned} W_1 &\rightarrow a_1 e^{i\tilde{\omega} \tilde{z}} + b_1 e^{-i\tilde{\omega} \tilde{z}} \\ W_2 &\rightarrow a_2 e^{i\tilde{\omega} \tilde{z}} + b_2 e^{-i\tilde{\omega} \tilde{z}} \end{aligned} \quad (\tilde{z} \rightarrow -\infty) \quad (A9)$$

where the incoming wave, $e^{i\tilde{\omega} \tilde{z}}$, arises entirely from the first term on the right-hand side of Eq. (A7), while the outgoing wave, $e^{-i\tilde{\omega} \tilde{z}}$, arises entirely from the second term. The coefficients in Eq.

(A9) are given by

$$\begin{aligned}
 a_1 &= e^{\frac{\pi}{2} \zeta \tilde{\omega}^{\frac{1}{2}}} \cdot \frac{\Gamma(1 - 2i\zeta \tilde{\omega}^{\frac{1}{2}}) \Gamma(-2i\zeta \tilde{\omega})}{\Gamma(-i\zeta \tilde{\omega}^{\frac{1}{2}} - i\zeta \tilde{\omega}) \Gamma(1 - i\zeta \tilde{\omega}^{\frac{1}{2}} - i\zeta \tilde{\omega})} \cdot e^{-\frac{\pi}{2} \zeta \tilde{\omega}} \\
 a_2 &= e^{-\frac{\pi}{2} \zeta \tilde{\omega}^{\frac{1}{2}}} \cdot \frac{\Gamma(1 + 2i\zeta \tilde{\omega}^{\frac{1}{2}}) \Gamma(-2i\zeta \tilde{\omega})}{\Gamma(i\zeta \tilde{\omega}^{\frac{1}{2}} - i\zeta \tilde{\omega}) \Gamma(1 + i\zeta \tilde{\omega}^{\frac{1}{2}} - i\zeta \tilde{\omega})} \cdot e^{-\frac{\pi}{2} \zeta \tilde{\omega}} \\
 b_1 &= e^{\frac{\pi}{2} \zeta \tilde{\omega}^{\frac{1}{2}}} \cdot \frac{\Gamma(1 - 2i\zeta \tilde{\omega}^{\frac{1}{2}}) \Gamma(2i\zeta \tilde{\omega})}{\Gamma(-i\zeta \tilde{\omega}^{\frac{1}{2}} + i\zeta \tilde{\omega}) \Gamma(1 - i\zeta \tilde{\omega}^{\frac{1}{2}} + i\zeta \tilde{\omega})} \cdot e^{\frac{\pi}{2} \zeta \tilde{\omega}} \\
 b_2 &= e^{-\frac{\pi}{2} \zeta \tilde{\omega}^{\frac{1}{2}}} \cdot \frac{\Gamma(1 + 2i\zeta \tilde{\omega}^{\frac{1}{2}}) \Gamma(2i\zeta \tilde{\omega})}{\Gamma(i\zeta \tilde{\omega}^{\frac{1}{2}} + i\zeta \tilde{\omega}) \Gamma(1 + i\zeta \tilde{\omega}^{\frac{1}{2}} + i\zeta \tilde{\omega})} \cdot e^{\frac{\pi}{2} \zeta \tilde{\omega}}.
 \end{aligned} \tag{A10}$$

To obtain Eqs. (40) and (41), we substitute Eq. (A10) into Eqs. (36) and (38), respectively, and make use of the recursion formula $\Gamma(z+1) = z \Gamma(z)$.

REFERENCES

- Campbell, W. H., "Studies of Magnetic Field Micropulsations with Periods of 5 to 30 Seconds," J. Geophys. Res., 64, 1819-1826, 1959.
- Campbell, W. H., "Natural Electromagnetic Field Fluctuations in the 3.0-to 0.02-cps Range," Proc. IEEE, 51, 1337-1342, 1963.
- Field, E.C., "Hydromagnetic Signals in the Ionosphere," The RAND Corporation, RM-3830-PR, September 1963.
- Field, E.C., private communication, 1964.
- Francis, W. E., and R. Karplus, "Hydromagnetic Waves in the Ionosphere," J. Geophys. Res., 65, 3593-3600, 1960.
- Greifinger, C., and P. Greifinger, "Low-frequency Hydromagnetic Waves in the Ionosphere," The RAND Corporation, RM-4225, October 1964.
- Hodder, D. T., R. A. Fowler, B. J. Kotick, and R. D. Elliott, "A Study of High Altitude Nuclear Blast Data," North American Aviation, Inc., SID 63-656, August 30, 1963.
- Horton, C. W., and A. A. J. Hoffmann, "Magnetotelluric Fields in the Frequency Range 0.03 to 7 cycles per Kilosecond, 1, Power Spectra," J. Res. NBS, 56D, 487-494, 1952.
- Jacobs, J. A., and T. Watanabe, "Propagation of Hydromagnetic Waves in the Lower Exosphere and the Origin of Short Period Geomagnetic Micropulsations," J. Atmos. Terrest. Phys., 24, 413-434, 1962.
- Maple, E., "Geomagnetic Oscillations at Middle Latitudes," J. Geophys. Res., 63, 1395-1404, 1959.
- Prince, C. E., Jr., and F. X. Bostick, Jr., "Ionospheric Transmission of Transversely Propagated Plane Waves at Micropulsation Frequencies and Theoretical Power Spectrums," J. Geophys. Res., 69, 3213-3234, 1964.
- Santirrocco, R. A., and D. G. Parker, "The Polarization and Power Spectrums of Pc Micropulsations in Bermuda," J. Geophys. Res., 68, 5545-5558, 1963.
- Smith, H. W., L. D. Provazek, and F. X. Bostick, Jr., "Directional Properties and Phase Relations of the Magnetotelluric Fields at Austin, Texas," J. Geophys. Res., 66, 879-888, 1961.